

Lattice and Siting Document

A. Chao, A. A. Garren, D. E. Johnson, S. Peggs, J. Sanford

December 15, 1988

Abstract

This is a status report of the lattice and the site adopted as of December 1988. In particular, the logic leading to the present lattice design, the possible lattice variations, and the tools developed for data handling and for site studies are discussed. How these results are to lead to the final construction lattice and footprint, however, is not discussed.

1. Lattice Design Decisions

A spectrum of different SSC lattices, and sections of lattices, has been designed and tested since—and before—the Central Design Group was founded four years ago. The lattice described in the Conceptual Design Report [1] incorporated most of the fundamental design decisions that have been adopted in subsequent lattice studies. The most important change made since then was to increase the betatron phase advance per cell from 60 to 90 degrees. This change, together with improvements in the IR optics, is included in the September 1987 lattice [2].

Some of the basic design decisions are mentioned briefly in the remainder of this section, and a more detailed discussion of the logic behind them is given in Appendix A. One of the lattices studied, the ISP lattice [3], will be described in section 2. This lattice, derived from the September 1987 lattice, has the significance that it fits the reference lattice footprint.

The magnets in the two SSC rings are magnetically and cryogenically independent, except around the Interaction Points (IPs) where the two proton beams pass through the same quadrupole magnets. The two beam lines are vertically separated by 0.7 meters, so that magnets for the two rings are located exactly one on top of the other. The polarity of vertically separated quadrupoles is different—a focussing (F) quadrupole in one ring lies on top of a defocussing (D) quadrupole in the other ring. [4,5]

"Spool pieces" in the regular cells are placed on the clockwise side of every quadrupole, forcing the dipoles to be asymmetrically placed relative to the quadrupoles. This breaks the overall mirror symmetry of the SSC slightly, but preserves the 180-degree rotational symmetry about the center of the ring.

The eight interaction and utility regions are not distributed uniformly around the ring. Instead, they are grouped in two "clusters" of four each, relatively close together. [6] This accounts for the approximately oval shape of the SSC footprint. Horizontal dispersion suppressors are included in every IR, in order to make the dispersion zero at the IPs. The spurious vertical dispersion introduced by the vertical beam separation is eliminated outside the separation region.

Interaction region (IR) quadrupoles have polarities which are antisymmetric relative to the IP. For example, if the IR quadrupole triplet on one side of the IP is FDF, the triplet on the other side is DFD. It is desirable to constrain the betatron phase advance between two low- β IPs, which can best be achieved by locating a pair of experimental IRs next to one another.

The distance between any two neighboring IPs (or centers of utility straight sections) in a cluster is the same, and is an integer times the regular arc cell length. In addition, all the IRs have the same horizontal bending geometry, which makes them fully modular—i.e., any two can be interchanged without modifying the beam line footprint. For example, "future" IRs in the cluster on the far side from the main SSC campus could easily be reconfigured from utility IRs to experimental IRs.

2. The ISP Lattice

When the Invitation for Site Proposals [7] (ISP) was written in April 1987, it was necessary to specify a reference lattice defining an exact footprint, which the states could investigate for compatibility with particular sites. That lattice, referred to here as the ISP lattice, is described briefly in this section and in more detail in Appendix B.

The major part of the 85.70-kilometer SSC circumference is contained in two arcs, as shown in Figure 1. Their main purpose is to provide most of the bending (313.2 degrees) necessary to close the ring, so they each consist simply of a large number of repeated cells. In between these two arcs are two clusters, under the main campus and on the far side of the SSC, each containing four IRs. A particular IR is used for injection or extraction, or contains an experiment. Clusters are joined to arcs by means of four "transition pieces," which consist of four cells identical to those in the main arcs, except that they have only a partial complement of dipoles. Their fundamental purpose is to allow for the possibility of bypasses, but they are also significant in decoupling optical and footprint perturbations.

A description of the optics and geometry of one of the 31.97-kilometer arcs reduces to the description of one of the 139.5 cells from which it is constructed. [8] A cell is composed of two half cells, which are geometrically identical, but which have quadrupoles of opposite polarities. A

114.57-meter half cell starts with a spool piece of total length 5.57 meters, which contains a variable combination of optical trim elements, cryogenic connections, and power supply feeds. It is followed by six dipoles, each of total length 17.34 meters, and finishes with a quadrupole package of length 4.96 meters, which includes a beam position monitor. The dipole field required at the maximum storage energy is directly proportional to the dipole bending angle

$$\theta = \frac{2\pi}{2*6*2*N_{\text{cells}} + 2*N_{\text{cluster}} + 4*N_{\text{tp}}} = \frac{2\pi}{3848} = 1.633 \text{ milliradians}$$

Here N_{cells} is the number of cells in an arc, and N_{cluster} and N_{tp} are the numbers of dipoles in the clusters and transition pieces, 194 and 28, respectively. The number of arc cells is adjusted to give a reasonable maximum dipole field, 6.586 tesla at 20 TeV.

There are three different kinds of IRs in the 9.05 kilometer clusters of the ISP lattice—two "low- β ," two "medium- β ," and four "utility" IRs. In order that such different IRs are compatible as a whole, they observe constraints on path length, phase advance, and bending angle. The IRs in a cluster are constructed so that the path length between any two neighboring IPs is exactly 10 times the cell length. Similarly, the distance between the end IPs of the two clusters, via one of the arcs, is exactly 157 cell lengths. Further, there are nominally exactly 48 bunches per cell, for a bunch spacing of 4.77 meters. These path-length modularities ensure that the bunch spacing can be multiplied by any cofactor of 48, while guaranteeing collisions at all IPs.

The two low- β experimental IRs are arranged as neighbors, with a betatron phase advance of an odd integer times $\pi/2$ between IPs. This leads to a desirable cancellation in the chromatic aberration which would otherwise exist around the whole of the SSC, due to the large β -functions at the strong quadrupole triplets. [6] The same arrangement is made with the medium- β IRs and the utility IRs, although the corresponding effects are much weaker.

The simplest way to guarantee closure is to insist that diametrically opposed IRs have identical dipole layouts. For example, the low- β IRs are opposite the medium- β IRs, and although the arrangement of quadrupoles is different in the two cases, the dipole arrangement is the same. Although it is not necessary that utility IRs have the same dipole arrangement as the experimental IRs, since identical utility IRs are diametrically opposed, this is the case in the ISP lattice.

Each 0.92-kilometer transition piece consists of two identical sequences of four half cells. This arrangement ensures that there is no exterior effect on the dispersion function due to the missing dipoles—instead of six dipoles in each half cell, there are six in the first two, two in the third, and none in the fourth. In regular SSC operation the beam passes through 28 dipoles in a transition piece, but in a bypass mode the transition piece is fitted with a full complement of 48 dipoles.

3. Adapting a Lattice to the Site

Having established the approximate location of the site, it is necessary to understand and control the inevitable rounds of minor layout adjustments to come. These adjustments will be driven not only by the need to avoid or approach prominent features on the chosen SSC site, but also by changes in the optical layout of the accelerator. There are several things which may be done in the lattice design to modify its shape and fit to a given footprint. These are listed below:

- Translate the plane of the lattice in all three dimensions in order to orient it to the footprint and to avoid obstacles.
- Rotate the plane of the lattice about its midpoint and tilt the plane to fit the terrain and geology.
- Change the average bending radius of the arcs. This can be done in two ways:
 - Change the normal cell length. This will involve rematching the optics, but is not a serious consideration in the lattice design.
 - Change the bend angle per normal cell and the number of normal cells. This can be done either by changing the number of dipoles per cell, or by changing the dipole field or length.
- Add empty cells or cells with missing dipoles in order to change the local bending radius of the lattice; however, certain constraints must be observed to avoid dispersion mismatches.
- Change the distribution of access points—i.e., have some cryogenic sectors with a different number of cells, in order to match the small land areas.
- Move dipoles around within the transition regions or change the distribution of dipoles between transition regions and the clusters, again observing certain constraints.
- Change the design of the cluster. This could take the form of:
 - changing the length of the straight sections
 - changing the number of straight sections per cluster
 - changing the amount of bending between the straight sections
 - adding additional transition regions, for example in the center of the cluster

These modifications could necessitate extensive optical redesigns, especially if used to decrease the overall cluster length.

- Put in a fold or hinge if it were needed in order to suit the terrain or geology

With this list of possible lattice modification tools, it should be possible to adapt the SSC lattice to any reasonable modifications of the ISP footprint.

4. Lattice Variations

At the present stage of lattice design, it is important to keep the flexibility for a range of possible lattice variations—deciding on a multipole correction scheme in the arcs, further optimization of IR optics, etc. The SSC lattices have been designed with this in mind. For example, the introduction of transition pieces more or less decouples the optics in the IRs and bypasses from that in the arcs. Thus it is hoped that early land-acquisition deadlines will not necessitate an early freeze of the optical design.

In this section, a list of examples of possible lattice variations studied in the past is given. They are grouped into two categories: bypasses and IR variants. Cell variations are not discussed. Variation of the cell structure is allowed provided of course the average bending curvature is maintained in the arcs.

Bypass Studies [9]

Many different bypass designs have been studied for the SSC lattice. The first was a bypass of the entire far cluster containing the two present and two future experimental areas [10]. Since that time, alternative bypass scenarios have been considered for bypassing one, two, or three straight sections [11]. The mechanics of all of these bypasses are essentially the same—they require the introduction of transition pieces, which allow the beams to be directed into either the main or the bypass leg, thus somewhat increasing the overall circumference of the machine. Within the bypass leg, every attempt has been made to duplicate the lattice structure found in the main leg—that is, the bypass leg consists of "insertion modules" composed of a horizontal dispersion suppressor, an experimental straight section, and another dispersion suppressor. There are several constraints which the bypass designs must satisfy:

- Both branches of the bypasses must have the same total horizontal bending
- There must be sufficient separation between the branches to allow independent operation
- The design must fit within the ISP footprint
- The linear optics of both branches must match the machine at the end of the bypasses

- The beam path length for both bypass legs must be carefully adjusted in order to assure collisions at all of the appropriate locations in both modes of operation. [12] While simultaneous collisions can be assured, the number of possible different bunch spacings could be substantially less in the bypass leg than in the machine without a bypass.
- The transition pieces must be duplicated on both sides of the machine in order to assure geometrical closure.

In addition to the above requirements, it is highly desirable that the straight part of the IR be at least 11 normal half cells in length overall, so that the same IR design could be used in either leg. Then any of the previously studied insertions desired could be used in the bypass with little or no modification.

The far cluster bypass satisfies all of the above. It fits within the ISP footprint, as the footprint was designed around it. Three options were considered for the bypass optics—(1) a simple beam bypass with no experimental areas, (2) a bypass with four possible experimental areas each the length of the standard design, and (3) a bypass with two experimental areas each twice the length of the standard design for special purpose experiments.

Two other "simple" bypass designs were studied, both of which fit into the ISP footprint: a bypass of two IRs and a bypass of a single IR. The double bypass has free regions of 11 and 15 half cells in the two legs and so causes no problems for the IRs. The single bypass has free spaces of 11 and 19 half cells, and thus would not require a new IR design. However, the path-length difference is very small in the single bypass and can not be made to produce collisions at all of the IRs without a reduction of about 10 percent in total luminosity.

Another type of bypass considered was the triple bypass, which could be used to have all of the experimental and utility straight sections on one side of the machine in a single campus. In order to maintain the same total number of straights, the cluster was increased from having two utilities and two IRs to having two utilities and two branches, each having three IRs. Here there were the additional options of having both utilities at one end of the bypass or having one utility at each end of the cluster. In either case, in order to fit into the footprint, the straight-section free space had to be reduced from 11 half cells to a mixture of 9, 10, and 11 half-cell lengths. These bypasses do require a redesign of both the utility and experimental straight sections. The 9 half-cell straights are rather small, and their linear optics, although adequate, are being compromised.

In the one-campus triple-bypass case, the three IRs in each leg could be any mixture of high or medium luminosity areas, with some cost to the expected machine performance. As mentioned before, a cancellation of certain chromatic effects can be obtained by having the two

low- β IRs run with the same value of β^* and with a betatron phase advance difference of an odd multiple of $\pi/2$. This cannot be done for all three of the triple-bypass IRs. Studies have been made on the consequences of not pairing the IRs, which show some detrimental effects, although these are not too serious [13].

Interaction Region Studies

The present two IR clusters have a modular design. Each cluster is composed of four modules, each of which is the length of 10 normal cells. Each module consists of a dispersion suppressor, some type of straight section which is free of horizontally bending dipoles, another dispersion suppressor, and three half cells. The purpose of this modularity is to allow a large degree of flexibility in the type of experimental or utility insertion which could be built into the cluster. Any type of module which is 10 cells long and has the same horizontal dipole distribution could be put into either cluster and still maintain the current lattice footprint. Several different experimental insertion designs have been investigated. While most of these obey the 10-cell rule, two do not. These two would require either the coalescing of two present IRs into one or the creation of a long bypass of one of the clusters. The various experimental insertions studied are listed in the following table:

| | β^* (m) | L^* (m) | Length | Reference | Comment |
|------------------------------------|--------------------------|------------|----------|-----------|---------|
| Low- β | 0.5–6.0 | ± 20 | 10 cells | [1] | |
| | 0.5–8.0 | ± 20 | 10 cells | [2] | |
| | late separation variants | | | [14] | |
| Low- β , high luminosity | 0.25–5.0 | ± 3 | 10 cells | [15] | (a) |
| Medium- β | 10–64 | ± 101 | 10 cells | [1] | |
| | 10–60 | ± 120 | 10 cells | [2] | |
| | late separation variants | | | [14] | |
| High- β , low p_T | 400–4000 | ± 12 | 10 cells | [16] | (b) |
| High rapidity | 206 | ± 182 | 10 cells | [17] | |
| | 1500–2000 | ± 750 | 14 cells | [18] | (c) |
| Very forward scattering experiment | 250–1000 | ± 1000 | 15 cells | [19] | (c) |

- a) This requires special high-gradient quadrupoles.
- b) $\theta_{\min} = 0.8 \mu\text{rad}$.
- c) This would require that either two IRs be coalesced into one or would need to be put into a bypass.

5. Analog Footprint

Following the development of the Conceptual Design for the SSC in 1986, it became necessary to express the land requirements to be provided by a state in proposing a site for the new facility. This effort took the form of a Siting Parameters Document, prepared by the CDG. [20] Portions of this document were used by DOE in preparing the Invitation for Site Proposals (ISP). [7] Certainly, one of the most important features was the graphical representation of the land requirements as expressed in the "Footprint" layout for the SSC.

The footprint was prepared based upon a conservative lattice, derived in late 1986. It incorporated a variety of assumptions, most of which have been described previously. Several representations of the calculated lattice geometry were considered. It was decided that a "four-parameter" characterization consisting of two radii and their corresponding turning points was adequate. By this device, it was possible to represent the geometry by an oval wherein the maximum deviation of the simplified representation from the true lattice was less than 30 feet.

The width and extent of the footprint were derived from operational considerations. Calculations were done concerning possible sources of radiation during routine and upset conditions of the facility. In order to provide a very adequate margin of safety, even under extreme conditions, the tunnel and all devices containing proton beams were surrounded with an amount of soil to attenuate any unwanted radiation from the accelerators. These determinations indicated the need for a band of land with a width of 1000 feet in the arc regions and somewhat more in the cluster areas. This ribbon of land was defined in a diagram, as shown in Figure 2, and by a table within the ISP. Provision of this ribbon by the states was requested by DOE in early 1987.

In addition to the diagram within the ISP, the states were provided with a mylar transparency, prepared by the RTK engineering firm, at a scale of 1:24000 that could be overlaid on a mosaic of USGS topographic maps in order to get an approximate representation of the SSC facility at the proposed site. This provided the basis for the states to use in their submittal of proposed sites in September 1987.

6. Digital Footprint

The previously described footprint became known as the "analog footprint," since it was based upon the radii and the turning points. It proved to be easy to use, and a suitable representation of the land requirements for the project at that time. The superimposition of the mylar layout on USGS maps gave an adequate illustration of a state's intentions in their proposal. The existing land features were readily identified and the overall site configuration could be ascertained.

As a next step in clarifying the land requirements, it is necessary to define the land requirements in terms of the precise location of the land boundaries for the SSC facilities. To achieve this objective, it is necessary to replace pictorial representations of the facility layout to one that is directly derivable from calculations - point by point. This leads to the "digital footprint," where the shape of the footprint is calculated based upon the locations of the more than 800 quadrupole magnets within the lattice.

The magnet locations are found by determining the x, y, and z positions of the center of each magnet within a rectilinear coordinate system whose origin is at a point to the lower left of the layout. The center of the footprint is at location (100000 ft., 100000 ft.) in plan view so that coordinate values of all components are positive. Using the lattice, a reference beam line, approximately oval, is then generated showing the tunnel and cluster locations as well as the land boundaries. For example, in the arc regions, the inner boundary is 150 feet inside the ring of magnets, while the outer boundary is 850 feet outside, for a total width of 1000 feet. Similar calculations determine the coordinates of all the major boundary markers of the injector, cluster, and service areas around the footprint.

An important step in the process is to express the land needs and boundary coordinates in terms that can be readily understood by state personnel who will be helping with land survey and land acquisition. It was decided with the assistance of RTK and their subcontractors to express the digital footprint in state plane coordinates for any of the Best Qualified List (BQL) sites. This coordinate system, adopted in 1927 and subsequently revised, allows for the projection of the land areas onto a plane with small, but known, distortions. It is intended that the use of the state plane coordinate system will be suitable for the purposes of land acquisition. However, it is not intended that this representation be used for determining the accurate alignment of the tunnel, let alone the precise location of accelerator components.

In generating the digital footprint for the site near Dallas, Texas, the digital lattice, as represented by the quadrupole magnet locations, was transferred electronically to the RTK computers. From there the lattice coordinates were transformed into state plane coordinates taking into account the location and orientation of the proposed collider ring (See Figure 3). The computer is the one used by RTK's Intergraphics CAD/E system and is well suited to creating the digital map of the footprint. The CAD/E system has the capability of creating various overlays of graphical information for subsequent studies.

One of the initial studies that will be undertaken concerns the mitigation of adverse impacts of the SSC upon the land and environment in the vicinity of the project facilities. This subject has been described in detail in the Final Environmental Impact Statement (FEIS) [21] prepared for the

siting decision and will be the primary topic of the site-specific EIS in 1989. Another important subject concerns the verification of the location of specific land parcels required for the project. This can now be done by the state surveyors guided by the accurate representation of the SSC project as expressed in the state plane coordinates.

7. Data Handling and Site Studies Tools

In order to assure a flexible, rapid response to lattice adjustments, both geometric and optical footprint information, in both local and state coordinates, must not only be available, but also be readily regenerated. Various software, hardware, and organizational tools have been developed with this end in mind.

Four sets of lattice database structures have been built, under a commercial relational database management system, as primary arrangements of data in the development of SSC lattices and footprints. While databases can be downloaded into ASCII files, in practice the available database management utilities make the information much more useful.

The first database structure is for "hierarchical" lattice optics, in a form organized for convenient lattice design. The second structure is a set of "flat" lattice optics tables, intended for general use when the lattice is viewed as a sequential list of elements. The third structure consists of lattice survey tables, which describe the local beam-line coordinates. Finally, the state planar structure represents the footprint, including both beam line and land acquisition information, in coordinates that surveyors find useful. More database structures will need to be added as time goes by—for example, describing the precise location of SSC objects in a yet-to-be-developed, site-wide coordinate system.

The databases are connected to the everyday computing environment, on the Sun workstations or on the LBL VAXs, via the Self DeScribing Dataset (SDS) libraries. Programs can read, write, or update databases in much the same way that files are accessed.

One program, DBSF, reads a set of hierarchical databases, and produces lattice information for use by particle tracking, lattice design, or other codes. The user can request output either as standard format or flat format ASCII files, as SDS datasets, or as flat database tables. Another program, FLAT, reads flat ASCII files, and outputs SDS datasets, or flat database tables. Connection from the flat database tables to the lattice survey tables is made by the program SURVEY, which can also read flat ASCII files, and can output ASCII survey files.

Lattice coordinate survey information is transformed into state planar information on RTK computers, necessitating the transmission of quite large ASCII files between the general CDG computing environment and RTK. These transfers are performed using a 9600-baud connection

between a Sun workstation and a CDG Intergraphics workstation, which in turn is connected via a 56-kbaud dedicated phone line to RTK.

With the information stored in the CAD/E system, it is possible to superimpose various layers of site-specific information. One layer may concern electrical power distribution while another may contain information on environmental concerns. As a result of studying such layouts, a movement of the entire footprint on the proposed region may be indicated. By understanding accurately the location of any problem to be avoided, an appropriate adjustment of the ring may be feasible.

Other studies may include a determination of the impact of different, perhaps more current lattice concepts within the site boundaries as defined by the ISP footprint. With the ability of the CAD/E system to "zoom in" on any specific region around the ring, it is possible to understand the impact of potential changes. If necessary, a totally new footprint can be created and its relationship to the one in the ISP studied. But, most importantly, the land and environmental consequences of any changes can be accurately examined.

References

1. Conceptual Design of the Superconducting Super Collider, SSC-SR-2020 (1986).
2. A. A. Garren and D. E. Johnson, The 90-degree (September 1987) SSC Lattice, SSC-146, (1987).
3. S. Peggs and D. E. Johnson, private communications.
4. P. Limon, Workshop Report on SSC Commissioning and Operations, SSC-5 (1985).
5. Report of the Workshop on Realistic SSC Lattices, SSC-SR-1015, Nov. 1985.
6. The Clustered Interaction Region Option for the SSC, SSC-SR-1014, Sept., 1985.
7. Invitation to Site Proposals for the SSC, DOE/ER-0315, April 1987.
8. The convention of breaking down the design into arcs, transition pieces and IRs may be different from that adopted in other reports, leading to some variation in the number of cells in each lattice segments. The lattice as a whole, however, should be the same in all reports.
9. M. G. D. Gilchriese and D. E. Johnson, Status Report on Bypass Studies for the SSC, SSC-N-565 (1988).
10. D.E. Johnson, "A Possible Beam Bypass for the SSC Clustered IR Region," *Proceedings of the 1986 Snowmass Summer Study*, 515 (1986).
11. A. A. Garren and D. E. Johnson, private communications. Also papers by (1) L. Lederman, "A One-lab SSC Configuration," *Proceedings of the 1986 Snowmass Summer Study*, 518 (1986); (2) L. Teng, "Studies of One-campus and Two-level Configurations for the SSC," SSC-N-506 (1988); and (3) T. Toohig, private communication. These studies have not been shown to fit within the ISP footprint.
12. D. E. Johnson, J. M. Peterson, and M. Tigner, Choice of the Accelerating Frequency in the SSC, SSC-N-117 (1986).
13. A .A. Garren and D. E. Johnson, Status of the SSC Lattice Design, SSC-151. A. A. Garren and D. E. Johnson, Chromatic Properties of the 90-degree (September, 1987) SSC Lattice, SSC-N-375.

14. S. Peggs, Segment Data for "Late Separation" Optics, SSC-N-65 (1985).
S. Peggs, Closed Luminosity and Injection Optics in a "Late" Separation Scheme for the SSC, SSC-N-87, (1985).
15. A. A. Garren, D. E. Johnson, and W. Scandale, "Layout and Performance of a High-Luminosity Insertion for the SSC, SSC-139 (1987).
16. D. E. Groom, A. A. Garren, and D. E. Johnson, "A Very Large Interaction Region for the SSC," *Proc. of the 1987 IEEE Particle Accelerator Conference*, 97 (1987).
17. A. A. Garren, private communication.
18. E. D. Courant, et al., "Summary Report of the IR Working Group," *Proc. of the 1986 Summer Study on the Physics of the Superconducting Super Collider*, 503 (1987).
19. D. E. Johnson and T. E. Toohig, "A Design for a 2-km Experimental Straight Section for the SSC," *Proc. of the 1987 IEEE Particle Accelerator Conference*, 89 (1987).
20. J. Sanford, SSC Siting Parameters Document, SSC-15 (1985).
21. Final Environmental Impact Statement of the SSC, DOE/EIS-0138, December 1988.
22. A. Garren, private communications (1988).
23. SSC Aperture Estimate for Cost Comparisons, SSC-SR-1013, Sept. 1985.
24. Optimization of the Cell Lattice Parameters for the SSC, SSC-SR-1024, Oct. 1986.
25. Report of the Reference Designs Study Group on the Superconducting Super Collider, May 1984.
26. F. Dell, *IEEE Trans. Nucl. Sci.*, NS-32, 1623 (1985).

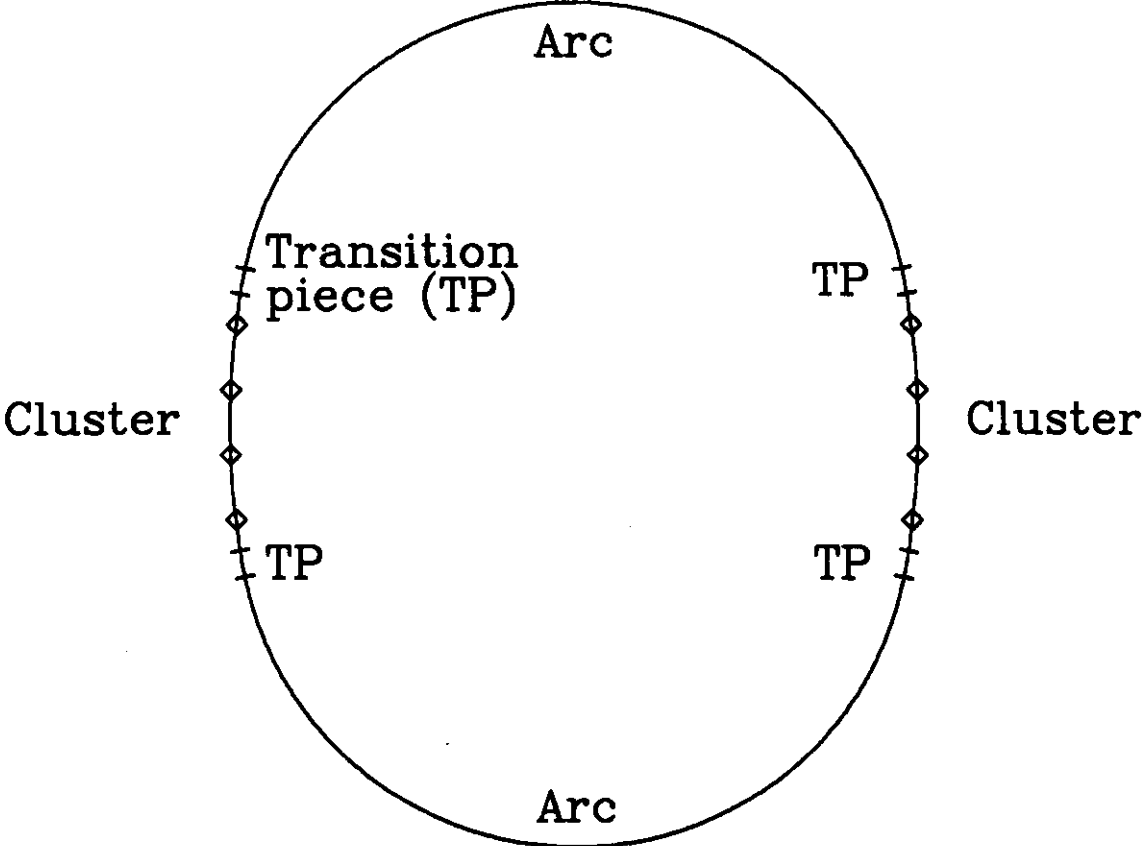


Figure 1. Beam line layout of the ISP lattice.

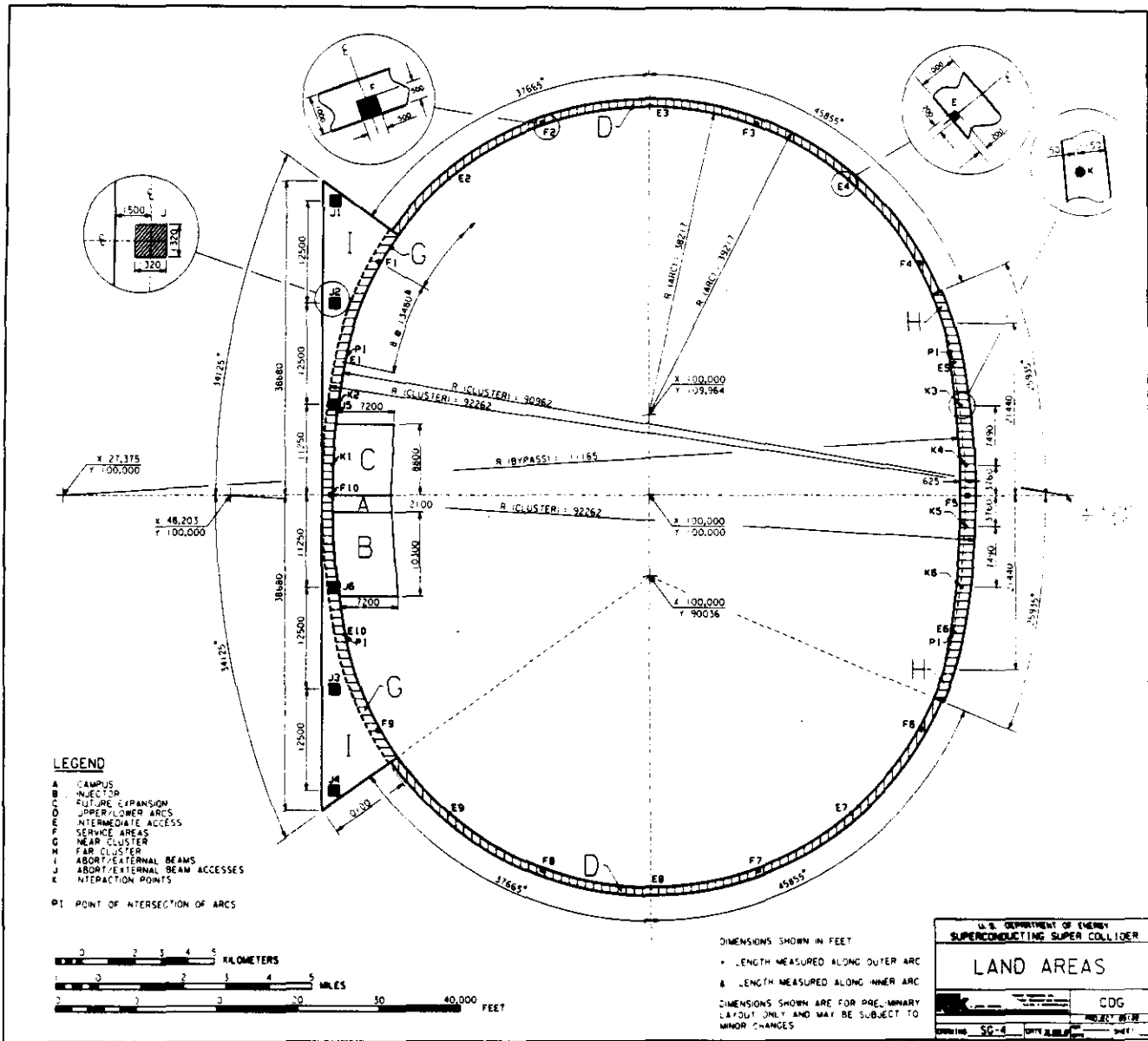


Figure 2. The ISP footprint.

Appendix A

Logic of Lattice Design Decisions

The ISP lattice design [3] evolved out of the design in the Conceptual Design Report [1] and has incorporated a number of fundamental design decisions. The major choices and the motivations leading to these choices are described in this appendix.

Magnets—Two-in-One vs. One-in-One Design

The decision to design the SSC lattice using magnetically and cryogenically separate magnets (one-in-one design) was based both on the expectation that separate magnets would be easier to construct and on the desire to be able to operate one ring independently of the other ring. While this cannot strictly be done in the present design, due to the common IR quadrupole triplets, the two rings offer much more flexibility than would be obtained with a two-in-one magnet design. [4] The cost of this decision is an increase in the magnet cost, and in the complexity of the beam crossing design, as the standard beam-beam separation is 70 cm instead of 15 to 20 cm in the two-in-one magnet designs. A preliminary study indicates that the 70-cm separation could perhaps be increased to 80 cm if desired. [22]

Normal Cell Design

The normal cells in the present design have a betatron phase advance of 90 degrees per cell. They are standard FODO cells, with six dipoles per half cell. The dipoles are clustered toward one end of the half cell in order to make space next to one side of each quadrupole for a spool piece containing power leads, cryogenic connections, and correction elements. This particular cell design was the result of several studies and optimizations [23, 24]. The decision to switch from the 60-degree cells of the CDR to the present 90-degree cells was due to a slight improvement in the usable aperture in the presence of dipole multipole errors.

Clustered vs. Distributed IRs

The lattice design in the RDS [25] had evenly distributed identical IRs, in order to obtain the highest amount of symmetry, and thus the most forgiving machine. It was felt at the time of the RDS design that the major aperture limitations to the SSC would be due to the large chromatic effects coming from the IR triplet quadrupoles, and that the easiest way to minimize these effects would be to cancel them as quickly as possible. It was realized, however, that it would be very

desirable to arrange the IRs in clusters in order to more efficiently use the campus areas, mechanical facilities, etc.

Following the RDS, a study was undertaken to examine the clustered vs distributed options [6]. The major results of this study were that the random dipole multipole errors dominated the usable aperture and diminished the advantage gained by any distributed symmetry, and that most of the chromatic effects of the IRs could be better offset by properly phasing the IRs with respect to each other than they could by individually correcting them with "local" sextupoles. Hence it was decided to design the SSC lattice with two long, clustered regions of straight sections both for the practical considerations of better facility utilization, and for the optical considerations of being better able to handle the non-linear IR chromatic effects.

Crossing Geometry—Vertical vs. Horizontal

The two proton rings can be situated either side-by-side or above and below one another. Correspondingly, the beams cross each other either horizontally or vertically at the IPs of the experimental IRs. Both possibilities have been explored. The present design adopts the vertical separation scheme.

Horizontal crossings were used for the RDS, a choice that was driven by the magnet choice of two-in-one; the fields of two-in-one magnet coils reinforce each other when horizontally separated and compete when vertically separated. Also, with the two beams so close, dispersion suppression was simpler with horizontal crossings. A complication of the horizontal crossings is the difficulty of assuring synchronization of the colliding bunches. A reasonable solution was found for this problem in the RDS since it had a distributed arrangement of IRs, but it would be much more awkward with a clustered lattice.

After it was decided to use separate magnets in separate cryostats for the two rings, the question arose anew. The strongest reason for the choice of vertically separated rings is the efficient use of tunnel space. Bunch synchronization is almost as compelling, especially with clustered insertions; with horizontal crossings, the inner and outer arcs have different lengths and one beam has both outer arcs, the other both inner arcs. A third argument has to do with simplicity and modularity. With vertical ring separations the two rings become virtually identical, and many parts of each ring are identical to each other. With horizontal ring separations there would be important differences between the inner and outer arcs, inner and outer dispersion suppressors, etc. One argument against vertical crossings is the need to include vertical dispersion suppressors.

Lattice Symmetry

The SSC lattice incorporates two important symmetries, which greatly simplify the design.

The first symmetry, which helps make the two rings identical, places identical strength magnets of the two rings directly above and below each other, but a focussing quadrupole of one ring is above or below a defocussing quadrupole of the other ring. This symmetry is almost inevitable because both beams go through common quadrupole triplets near the crossings, where they see opposite focussing due to their opposite velocities.

The second symmetry is that the optical focussing pattern in a straight section reflects antisymmetrically about its center. Thus, each beam encounters identical-strength opposite-gradient quadrupoles at equal distances from the IP on the left and right sides. This symmetry, together with the first one, assures the identity of the two rings. It also simplifies the β -function matching; it suffices to match from the cells to the IP on one side and that of the other follows automatically. Moreover, since the horizontal and vertical β -functions are interchanged on the two sides, the phase advances through the entire insertion are the same. This makes it possible to obtain the proper phase advance between adjacent IPs in both transverse planes, which is desirable to reduce chromatic perturbations caused by the low- β triplets.

There is a possible alternative to the second symmetry. Rather than making the IR straight sections antisymmetric about the IPs, they could be symmetric. The two members of each pair of IRs would be given opposite polarities. Within each IR the two beams would have opposite polarities, due to the first symmetry. The two IR modules of a pair would no longer be identical, but would have opposite polarities. This scheme, which might be called the third symmetry, amounts to a rearrangement of components of a lattice that uses the second symmetry. In fact, there are no physical differences between the two, only a permutation of the signs of various gradients. Both the second and third schemes preserve overall identity of the two rings and proper phase relations between IPs. However, if one ever wished to have different β^* values in the two members of a pair, the beam-to-beam identity would disappear.

Tune Adjustment Ability

Two of the lattice designs in the RDS adjusted the overall tune of the machine by changing the tunes of the individual normal cells, while the other design made use of special "phase trombones"—a short section of special cells which could be tuned over a large range of phase advances while not changing the linear optics outside of that section. This was considered advantageous in that design as it totally decoupled the machine's operating point and the optics of the IRs. In particular, it allowed the IRs' β^* to be adjusted over a very large range (e. g., 1 m to

100 m) without having to compensate for the tune change in the rest of the ring. These phase trombones were initially considered for the SSC [5].

In subsequent designs the phase trombones were dropped in order to increase the simplicity and overall efficiency of the lattice. It was decided that the desired tuning range of an IR was roughly a factor of ten rather than several hundred, and IR designs which could be tuned over this range without changing their phase advance were found. Because of these designs, the necessary tuning ability of the SSC is quite small, ≈ 2 -3 units, which can easily be handled with quadrupole correction elements in the arc cells, with an almost unnoticeable effect on the machine optics.

Modularity of Straight-Section Insertions

The SSC lattice as presently conceived has four pairs of straight sections: utility, low- β high-luminosity IRs, medium- β lower-luminosity IRs, and "future" IRs. The latter are identical to utility straight sections, but could be rebuilt later as IRs. Crossings occur in the IRs but not in the utility or future IRs.

Each straight section is grouped with a dispersion suppressor on each side and three normal half cells into a cluster module. All of the cluster modules are identical except for the internal structure within each straight section, and all are matched to the arc cells with respect to all orbit functions. Each straight section has the length of 11 half cells; each dispersion suppressor is 3 half-cells long, giving a module the length of 10 cells, or 2285 m.

There are three main reasons for this modularity. First, it permits a high degree of operational flexibility. Thus the "future" IRs, initially configured as utility straight sections, can later be reconfigured as real IRs without lattice changes in the rest of the ring. Second, it makes it easier to achieve the correct phase advance between the members of all pairs of identical straight sections. Third, the lattice is simplified in that the number of different components is minimized. The lattice will have many regularities, making it easier to understand and operate.

Dispersion Suppressors

Dispersion suppressors are needed to change the dispersion—i.e., the off-energy function—from its characteristic non-zero value in the arc cells to zero value in the experimental and utility straight sections. This is done so that the dispersion is properly matched in the arcs—which is the way to minimize its maximum values and to make it periodic, to minimize beam size at the collision points which maximizes luminosity, and to simplify the optics of β -function matching of the insertions, since that problem is thereby decoupled from that of dispersion matching. It is

especially important that the dispersion be properly matched in the arc cells, to minimize aperture requirements and nonlinear perturbations of off-energy particles.

Three types of dispersion suppressors have been used in SSC design studies. The first, used for the RDS [25], was a missing magnet type. Such a suppressor consists of a number of normal cells with dipoles removed in a certain pattern. This type has the virtues of not perturbing the β -functions and simplicity; the disadvantage is that the circumference of the ring is increased.

A second type, used for the CDR [1], consisted of three cells with normal bending but altered quadrupole strengths. This type uses circumference more efficiently; however, it has additional quadrupole circuits or lengths and it does slightly perturb the β -functions.

The third type, which is presently favored, was invented for use in the 90-degree (September 1987) Lattice [2]. It consists of two 90-degree cells, each having three-quarters the length and two-thirds the bending of a regular cell (4 dipoles per half cell vs. 6). This type is simple, compact, and does not perturb the β -functions, leading to cleaner optics in the experimental IRs.

Interaction Region Design

There are four experimental IR straight sections in the SSC lattice, grouped into two pairs. There are two adjacent low- β IRs in the near cluster and two adjacent medium- β IRs in the far cluster. Both kinds have the same structure, but various magnet and drift lengths are different. These straight sections have three main requirements: to produce the desired β^* values for the experiments, to be tunable to a gentler optics for injection, and to provide the mechanism for the crossings. The latter is achieved by a separate set of non-tunable magnets, which have no direct effect on the β -function tuning and matching.

The crossings are done in a stepwise fashion with a region centered at the IP in which the two beams are colinear. On either side of the IP in this colinear region there is a drift space of length L^* followed by a quadrupole triplet. The detectors are located about the IP in the drift spaces, which have a length $L^* = 20$ m in the low- β IRs and $L^* = 120$ m in the medium- β IRs. These lengths differ because of the different types of events the detectors are designed to record, and the necessity of having the triplets close to a low- β IP to get the β values under control quickly.

Minimum β^* Value

The minimum value for β^* for the high-luminosity insertions has been chosen to be 0.5 m. This is believed to be close to the tightest focussing allowed by the present quadrupole technology.

While other proton accelerators have achieved such values of β^* , because of their higher effective quadrupole gradients due to their lower energies, they have run with substantially smaller values of maximum beta (1.1 km at Fermilab vs. ≈ 8 km for the SSC). Extensive tracking studies on the SSC indicate that this very large beta value is acceptable provided that the IR quadrupoles are individually measured and that the first five normal and skew multipoles are corrected to 90 percent. [26] One design yielding $\beta^* = 0.25$ m with the same value for beta-max has been investigated, but this design requires quadrupoles with still higher gradients and reduces the available free space from ± 20 m to ± 3 m.

β -function Tuning

The β -function matching between the IP and the beginning of the dispersion suppressor is done with six quadrupoles, Q1-Q6. The central triplet, Q1, Q2, Q3, is common to both beams. There is a long space between Q3 and Q4. Q4 and Q5 constitute a doublet, and Q6 is some distance from Q5. Q5 and Q6 have the same polarity, and tuning between injection and experimental optics is done by gradually strengthening Q6 and weakening Q5, with small changes in the gradients of Q1-Q4. The tuning range of β^* is from 8 m to 0.5 m in the low- β IR and from 60 m to 10 m in the medium- β IR.

Crossings

The two proton beams are separated by 70 cm in the arcs, and cross from top to bottom and vice versa in the IR straight sections. The crossings are done in four steps, two steps in each Q3-Q4 space, causing the beams to be nearly colinear through the triplets and the central drift space that contains the detectors. With this scheme, the beams are separated as close to the IP as possible, which minimizes long range beam-beam effects.

Vertical Dispersion Matching

The vertical bending magnets that cross the beams give rise to vertical dispersion. By placing two vertical steps in each Q3-Q4 space and separating these by a special quadrupole structure, it is possible to have zero vertical dispersion both in the arcs and in the colinear triplet-detector region. The special structure consists of two very short 90-degree cells, giving it a -1 transfer matrix. This $M = -1$ matrix section exactly compensates the dispersion introduced by the two steps. Since it is invisible to the β -function, the tuning by Q1-Q6 described above is unaffected.

Alternative Crossing Dispersion-Matching Schemes

The $M = -1$ vertical dispersion matching section described above contains eight long, strong quadrupoles, which makes it tempting to seek a better solution. One such alternative has been proposed, [14] which consists of extending the colinear region through Q5, disposing of Q6, and then placing the vertical steps in the horizontal dispersion suppressor such that both dispersions are matched there. The advantage of this scheme is avoiding the $M = -1$ quadrupoles. One potential disadvantage is an increase in the long range beam-beam interaction. It remains to be demonstrated whether the injection-collision tuning could be done as simply with this approach as with that explained above, and that it fits the ISP footprint.

Transition Regions

The lattice design for the ISP footprint includes, at each end of each cluster region, transition regions, to allow for the future possibility of adding one of the various beam bypass options. These transition regions each consist of four regular cells which are approximately half-filled with dipoles. The partially empty cells are required in order to be able to switch from one beam configuration to the other without moving magnets. At the beginning of the transition region, the beam goes through a few dipoles which are not powered in normal operation. The switching from the main channel to the bypass channel is done by powering these dipoles. The cost of including the bypass potential, because these cells are partially dipole free, is to increase the overall machine circumference by some eight cell lengths, or ≈ 1825 m.

Appendix B

Details of the ISP lattice [3] are given in this appendix.

APPENDIX 2 DESCRIPTION OF THE ISP LATTICE

Dec 16, 1988

This appendix is broken into six sections, corresponding to the six database tables which describe the ISP lattice. Each section is derived from an ASCII dump of one table, with only minor editing changes made for reading ease.

The first section (table), BEAM_LINE, describes large structures in the lattice, such as clusters, arcs, sectors, or cells.

The second section, IDEAL_MAGNET, describes the set of physical magnets - magnets with field free ends, et cetera, as they would be installed in the SSC.

The third section, MAGNET_PIECE, contains the elements from which complete magnets are constructed. An IDEAL_MAGNET quadrupole, for example, includes field free ends, a marker at its center, two halves with fields, and a beam position monitor.

The fourth section, STRENGTH, lists those magnet strengths which can be varied by changing a current on a bus. The actual values correspond to a luminosity lattice.

The fifth section, GEOMETRY, describes those parameters which are fixed after magnets have been installed. Examples are the number of dipoles in a half cell, the dipole bending angle, and the free space in an intersection region.

The sixth section, NAME_LOCATION, is an index of object names, listing the name of the table in which that object may be found. For example, SBC-TORA is found in BEAM_LINE, and PI is found in GEOMETRY.

| Section 1 | BEAM_LINE | Constituents |
|---|----------------------|--------------|
| bds1 | dds1a 4*dipole dds1b | |
| Bending section in the 1st half cell of a dispersion suppressor | | |
| bds2 | dds2a 4*dipole dds2b | |
| Bending section in the 2nd half cell of a dispersion suppressor | | |
| bds3 | dds3a 4*dipole dds3b | |
| Bending section in the 3rd half cell of a dispersion suppressor | | |

bds4 dds4a 4*dipole dds4b
 Bending section in the 4th half cell of a dispersion suppressor

celldd hcellfd hcellfd
 A main arc cell, broken between the D quad and the D spool piece

cellff hcellfd hcellfd
 A main arc cell, broken between the F quad and the F spool piece

converge spool dipoles per hcell*dipole mtpcon 2*(celldd dtof24 mtfod) mtpcon
 A bypass could CONVERGE with the main ring here, using bend modified cells

d w diverge dsd
 Transition piece from sector D to straight W, at the start of the FAR cluster

diverge mtpdiv 2*(mtfod dtof42 cellff) mtpdiv spoolf
 dipoles_per_hcell*dipole
 A bypass could DIVERGE from the main ring here, using bend modified cells

down_lb1 mlbstep dip_d_lb1 dstep dip_d_lb1 mlbstep
 Downward vertical bend in inner low beta step

down_lb2 mlbstep dip_d_lb2 dstep dip_d_lb2 mlbstep
 Downward vertical bend in outer low beta step

down_mb mmbstep 3*(dip_d_mb dstep) dip_d_mb mmbstep
 Downward vertical bend in medium beta step

dsd ~qhybd dsdcore dsend
 Dispersion suppressor, with end quadrupoles, from D to D

dsdcore bds1 qdsf bds2 qdsd bds3 qdsf bds4
 Core of the D Dispersion suppressor, without end quadrupoles

dsf dsend dsfcore qhybf
 Dispersion suppressor, with end quadrupoles, from F to F

dsfcore bds1 qdsd bds2 qdsf bds3 qdsd bds4
 Core of F Dispersion suppressor, without end quadrupoles

dtof24 empty_spool 2*dipole 4*empty_dipole quad90f
 Main ring part of a switch for a possible bypass

dtof42 empty_spool 4*empty_dipole 2*dipole quad90f
 Main ring part of a switch for a possible bypass

far d_w strait_w_x strait_x x_y strait_y y_z strait_z
 z_e
 The cluster FAR from the main campus, with no injectors

fdfd cellff spoolf dipoles per hcell*dipole
 A transition piece from D to F, NOT using physical magnets

h_q diverge dsd

Transition piece from sector H to straight Q, at the start of the NEAR cluster
 hcellidf spoold dipoles_per_hcell*dipole quad90f
 Half a main arc cell, from D to F locations
 hcellidf spoolf dipoles_per_hcell*dipole quad90d
 Half a main arc cell, from F to D locations
 hmlcellidf dml gmlf dml
 Half cell of "M = -1" section, with a DF doublet sandwiched between drifts
 hmlcellidf dml gmlf gmlf dml
 Half cell of "M = -1" section, with a FD doublet sandwiched between drifts
 lb0d3 dlbstar qlbd1 qlbf2 dlb2 qlbf2 qlbd3
 Low beta front end, from IP to end of DFD triplet
 lb0f3 dlbstar qlbf1 qlbd2 dlb2 qlbd2 qlbf3
 Low beta front end, from IP to end of DFD triplet
 lb down_d lb0d3 step_d lb1 minusl_f step_d lb2 lb0d4d6
 Half a dropping low beta straight, from IP to D exit
 lb down_f lb0f3 step_d lb1 minusl_d step_d lb2 lb0f4f6
 Half a dropping low beta straight, from IP to F exit
 lb up_d lb0d3 step_u lb1 minusl_f step_u lb2 lb0d4d6
 Half a rising low beta straight, from IP to D exit
 lb up_f lb0f3 step_u lb1 minusl_d step_u lb2 lb0f4f6
 Half a rising low beta straight, from IP to F exit
 lb0d4d6 qlbd4 dlb45 qlbf5 dlb56 qlbd6
 Last 3 quads in low beta focussing, quads 4 to 6, D to D
 lb0f4f6 qlbf4 dlb45 qlbd5 dlb56 qlbf6
 Last 3 quads in low beta focussing, quads 4 to 6, F to F
 left sector_a sector_b sector_c sector_d
 The main arc on the left, looking from the NEAR cluster to the FAR cluster
 mb0d3 dmbstar gmbd1 gmbf2 dmb2 gmbf2 gmbd3
 Medium beta front end, from IP to end of DFD triplet
 mb0f3 dmbstar gmbf1 gmbd2 dmb2 gmbd2 gmbf3
 Medium beta front end, from IP to end of DFD triplet
 mb down_d mb0d3 step_d mb minusl_f step_d lb2 mbd4d6
 Half a dropping medium beta straight, from IP to D exit
 mb down_f mb0f3 step_d mb minusl_d step_d lb2 mb0f4f6
 Half a dropping medium beta straight, from IP to F exit
 mb up_d mb0d3 step_u mb minusl_f step_u lb2 mbd4d6
 Half a rising medium beta straight, from IP to D exit

mb up_f mb0f3 step_u mb minusl_d step_u lb2 mb0f4f6
 Half a rising medium beta straight, from IP to F exit
 mbd4d6 gmbd4 dmb45 gmbf5 dmb56 gmbd6
 Last 3 quads in medium beta focussing, quads 4 to 6, D to D
 mb0f4f6 gmbf4 dmb45 gmbd5 dmb56 gmbf6
 Last 3 quads in medium beta focussing, quads 4 to 6, F to F
 minusl_d hmlcellidf hmlcellidf hmlcellidf dml gmlf gmlf
 D to D "M = -1" section: two cells with missing DMI drift at downstream end
 minusl_f hmlcellidf hmlcellidf hmlcellidf dml gmlf gmlf
 F to F "M = -1" section: two cells with missing DMI drift at downstream end
 mtftod empty_spool dipoles_per_hcell*empty_dipole quad90d
 Half a main arc cell, from F to D locations, with empty dipole and spool slots
 near h_q strait_q q_r strait_r r_s strait_s s_t strait_t
 t_a
 The cluster NEAR the main campus, where the injectors are.
 q_r dsf fdfd dsd
 Transition between straights Q and R, in the NEAR cluster
 r_s dsf fdfd dsd
 Transition between straights R and S, in the NEAR cluster
 right sector_e sector_f sector_g sector_h
 The main arc on the right, looking from the NEAR cluster to the FAR cluster
 s_t dsf fdfd dsd
 Transition between straights S and T, in the NEAR cluster
 sector_a hcellidf 15*celliff vsmc 18*celliff
 Sector A in the LEFT main arc
 sector_b 18*celliff vsmb 18*celliff
 Sector B in the LEFT main arc
 sector_c 18*celliff vsmc 18*celliff
 Sector C in the LEFT main arc
 sector_d 18*celliff vsmd 16*celliff
 Sector D in the LEFT main arc
 sector_e hcellidf 15*celliff vsme 18*celliff
 Sector E in the RIGHT main arc
 sector_f 18*celliff vsmf 18*celliff
 Sector F in the RIGHT main arc
 sector_g 18*celliff vsmg 18*celliff
 Sector G in the RIGHT main arc
 sector_h 18*celliff vsmh 16*celliff

Sector H in the RIGHT main arc

```

ssc_red      near left far right
One of two vertically separated complete storage rings
step_d_lb1   dblend down_lb1 dlbmid up_lb1 dlbend
Inner step down in a low beta straight, with no net vertical angle
step_d_lb2   dlb2end down_lb2 dlb2mid up_lb2 dlb2end
Outer step down in a low beta straight, with no net vertical angle
step_d_mb    dmbend down_mb dmbmid up_mb dmbend
Step down in a medium beta straight, with no net vertical angle
step_u_lb1   dblend up_lb1 dlbmid down_lb1 dlbend
Inner step up in a low beta straight, with no net vertical angle
step_u_lb2   dlb2end up_lb2 dlb2mid down_lb2 dlb2end
Outer step up in a low beta straight, with no net vertical angle
step_u_mb    dmbend up_mb dmbmid down_mb dmbend
Step up in a medium beta straight, with no net vertical angle

strait_q     -utility_f miputq utility_d
First utility straight, in the NEAR cluster

strait_f     -utility_f miputr utility_d
Second utility straight, in the NEAR cluster

strait_s     -lb_down_f miplbs lb_up.d
Low beta straight, with rising beam, in the NEAR cluster

strait_t     -lb_up_f miplbt lb_down.d
Low beta straight, with dropping beam, in the NEAR cluster

strait_w     -utility_f miputw utility_d
First undeveloped straight in the FAR cluster, configured as a utility

strait_x     -utility_f miputx utility_d
Second undeveloped straight in the FAR cluster, configured as a utility

strait_y     -mb_down_f mipmby mb_up.d
Medium beta straight, with rising beam tube, in the FAR cluster

strait_z     -mb_up_f mipmbz mb_down.d
Medium beta straight, with dropping beam tube, in the FAR cluster

t_a         dsf converge
Transition piece from straight T to sector A, at the end of the NEAR cluster

up_lb1      mlbstep dip_u_lb1 dstep dip_u_lb1 mlbstep
Upward vertical bend in inner low beta step

up_lb2      mlbstep dip_u_lb2 dstep dip_u_lb2 mlbstep
Upward vertical bend in outer low beta step
    
```

```

up_mb       mmbstep 3*(dip_u_mb dstep) dip_u_mb mmbstep
Upward vertical bend in medium beta step

utility_d    dutstar qutl1 dutl2 qutd2 dut23 qutf3 dut34 qutd4
Half a utility straight, intersection point to D exit

utility_f    dutstar qutd1 dutl2 qutf2 dut23 qutd3 dut34 qutf4
Half a utility straight, from intersection point to F exit

w_x         dsf fdfd dsd
Transition between straights W and X, in the FAR cluster

x_y         dsf fdfd dsd
Transition between straights X and Y, in the FAR cluster

y_z         dsf fdfd dsd
Transition between straights Y and Z, in the FAR cluster

z_e         dsf converge
Transition piece from straight Z to sector E, at the end of the FAR cluster

*****
Section 2    IDEAL_MAGNET
Format:
    
```

| Ideal magnet name | Constituents |
|--|----------------------------|
| dip_d_lb1 | dend bdownlb1 dend |
| Downward dipole in inner low beta step | |
| dip_d_lb2 | dend bdownlb2 dend |
| Downward dipole in outer low beta step | |
| dip_d_mb | dend bdownmb dend |
| Downward bend in medium beta step | |
| dip_u_lb1 | dend buplb1 dend |
| Upward dipole in inner low better step | |
| dip_u_lb2 | dend buplb2 dend |
| Upward dipole in outer low beta step | |
| dip_u_mb | dend buymb dend |
| Upward bend in medium beta step | |
| dipole | dend bend dend |
| Main arc horizontal dipole, with field free ends | |
| qdsd | dend hqdsd mads hqdsd dend |
| First quadrupole in the dispersion suppressor, D | |

qdsf dend hqdsf mqds hqdsf dend
 First quadrupole in the dispersion suppressor, F
 qhybd dend hqdsd mqds hqd90 dend
 Hybrid D quadrupole at the normal dispersion end of a dispersion suppressor
 qhybf dend hqdsf mqds hqf90 dend
 Hybrid F quadrupole at the normal dispersion end of a dispersion suppressor
 qlbd1 dend hqlbd1 mq1b hqlbd1 dend
 First (Defocussing) quadrupole in a low beta triplet
 qlbd2 dend hqlbd2 mq1b hqlbd2 dend
 Second (Defocussing) quadrupole in a low beta triplet
 qlbd3 dend hqlbd3 mq1b hqlbd3 dend
 Third (Defocussing) quadrupole in a low beta triplet
 qlbd4 dend hqlbd4 mq1b hqlbd4 dend
 Fourth (Defocussing) quadrupole in low beta optics
 qlbd5 dend hqlbd5 mq1b hqlbd5 dend
 Fifth (Defocussing) quadrupole in low beta optics
 qlbd6 dend hqlbd6 mq1b hqlbd6 dend
 Sixth (Defocussing) quadrupole in low beta optics
 qlbf1 dend hqlbf1 mq1b hqlbf1 dend
 First (Focussing) quadrupole in a low beta triplet
 qlbf2 dend hqlbf2 mq1b hqlbf2 dend
 Second (Focussing) quadrupole in a low beta triplet
 qlbf3 dend hqlbf3 mq1b hqlbf3 dend
 Third (Focussing) quadrupole in a low beta triplet
 qlbf4 dend hqlbf4 mq1b hqlbf4 dend
 Fourth (Focussing) quadrupole in low beta optics
 qlbf5 dend hqlbf5 mq1b hqlbf5 dend
 Fifth (Focussing) quadrupole in low beta optics
 qlbf6 dend hqlbf6 mq1b hqlbf6 dend
 Sixth (Focussing) quadrupole in low beta optics
 qmld dend hqmdl mqml hqmdl dend
 A Defocussing quadrupole in an "M = -1" section
 qmlf dend hqmlf mqml hqmlf dend
 A Focussing quadrupole in an "M = -1" section
 qmbd1 dend hqmbd1 mqmb hqmbd1 dend
 First (Defocussing) quadrupole in a medium beta triplet
 qmbd2 dend hqmbd2 mqmb hqmbd2 dend
 Second (Defocussing) quadrupole in a medium beta triplet

qmbd3 dend hqmbd3 mqmb hqmbd3 dend
 Third (Defocussing) quadrupole in a medium beta triplet
 qmbd4 dend hqmbd4 mqmb hqmbd4 dend
 Fourth (Defocussing) quadrupole in medium beta optics
 qmbd5 dend hqmbd5 mqmb hqmbd5 dend
 Fifth (Defocussing) quadrupole in medium beta optics
 qmbd6 dend hqmbd6 mqmb hqmbd6 dend
 Sixth (Defocussing) quadrupole in medium beta optics
 qmbf1 dend hqmbf1 mqmb hqmbf1 dend
 First (Focussing) quadrupole in a medium beta triplet
 qmbf2 dend hqmbf2 mqmb hqmbf2 dend
 Second (Focussing) quadrupole in a medium beta triplet
 qmbf3 dend hqmbf3 mqmb hqmbf3 dend
 Third (Focussing) quadrupole in a medium beta triplet
 qmbf4 dend hqmbf4 mqmb hqmbf4 dend
 Fourth (Focussing) quadrupole in medium beta optics
 qmbf5 dend hqmbf5 mqmb hqmbf5 dend
 Fifth (Focussing) quadrupole in medium beta optics
 qmbf6 dend hqmbf6 mqmb hqmbf6 dend
 Sixth (Focussing) quadrupole in medium beta optics
 qad90d dend hqd90 mq90 hqd90 bpm dend
 Defocussing main arc quadrupole, with a marker, a BPM, and field free ends
 qad90f dend hqf90 mq90 hqf90 bpm dend
 Focussing main arc quadrupole, with a marker, a BPM, and field free ends
 qutd1 dend hqutd1 mqut hqutd1 dend
 First (Defocussing) quadrupole in utility optics
 qutd2 dend hqutd2 mqut hqutd2 dend
 Second (Defocussing) quadrupole in utility optics
 qutd3 dend hqutd3 mqut hqutd3 dend
 Third (Defocussing) quadrupole in utility optics
 qutd4 dend hqutd4 mqut hqutd4 dend
 Fourth (Defocussing) quadrupole in utility optics
 qutf1 dend hqutf1 mqut hqutf1 dend
 First (Focussing) quadrupole in utility optics
 qutf2 dend hqutf2 mqut hqutf2 dend
 Second (Focussing) quadrupole in utility optics
 qutf3 dend hqutf3 mqut hqutf3 dend

Third (Focussing) quadrupole in utility optics
 qut4 dnd hqut4 mqut hqut4 dnd
 Fourth (Focussing) quadrupole in utility optics
 spoold hspool steer_d qtrimd sext_d empty_slot hspool
 Spool piece next to D quads in main arcs
 spoolf hspool steer_f qtrimf sext_f empty_slot hspool
 Spool piece next to F quads in main arcs

 Section 3 MAGNET_PIECE
 Format:

| Magnet piece name Comment | Type | Tilt | Length | Strength |
|--|--------|--------|-----------------|------------------------|
| bdown1b1 Downward bend in inner low beta step | s bend | 0.5*pi | lbvlb1 | bbvlb1*lbvlb1 / brho |
| bdown1b2 Downward bend in outer low beta step | s bend | 0.5*pi | lbfield | bbvlb2*lbfield / brho |
| bdownmb Downward bending field in medium beta step | s bend | 0.5*pi | lbvmb | bbvmb * lbvmb / brho |
| bend Magnetic part of a main arc dipole | s bend | | lbfield | bangle |
| bpm Beam Position Monitor, included with most quadrupoles | drift | | lbpm | |
| bup1b1 Upward bend in inner low beta step | s bend | 0.5*pi | lbvlb1 | - bbvlb1*lbvlb1 / brho |
| bup1b2 Upward bending field in outer low beta step | s bend | 0.5*pi | lbfield | - bbvlb2*lbfield/brho |
| bupmb Upward bending field in medium beta step | s bend | 0.5*pi | lbvmb | - bbvmb*lbvmb / brho |
| dds1a Drift A in the 1st half cell of a dispersion suppressor | drift | | lds1a | |
| dds1b Drift B in the 1st half cell of a dispersion suppressor | drift | | ldsfree - lds1a | |
| dds2a Drift A in the 2nd half cell of a dispersion suppressor | drift | | lds2a | |
| dds2b Drift at ends of medium beta step | drift | | ldsfree - lds2a | |

Drift B in the 2nd half cell of a dispersion suppressor
 dds3a drift lds3a
 Drift A in the 3rd half cell of a dispersion suppressor
 dds3b drift ldsfree - lds3a
 Drift B in the 3rd half cell of a dispersion suppressor
 dds4a drift lds4a
 Drift A in the 4th half cell of a dispersion suppressor
 dds4b drift ldsfree - lds4a
 Drift B in the 4th half cell of a dispersion suppressor
 dnd lnd
 Field free region at both ends of all(?) magnets

d1blend drift ldlblend
 Drift at ends of inner low beta step
 d1blend drift ldlblend
 Drift at middle of inner low beta step
 d1b2 drift ldlb2
 Spacer between two halves of middle quad in low beta triplet
 d1b2end drift ldlb2end
 Drift at ends of outer low beta step
 d1b2mid drift ldlb2mid
 Drift at middle of outer low beta step
 d1b45 drift 1lb46 - lqlb4tot - 2*1qlb5tot - ldlb5
 Drift between 4th and 5th quads in low beta optics
 d1b56 drift ldlb56
 Drift between 5th and 6th quads in low beta optics
 d1bstar drift 1lbstar - lnd
 Drift from low beta IP to inner edge of triplet
 dmb1 drift ldm1
 Half of the drift between adjacent "M - J" quadrupole doublets
 dmb2 drift ldm2
 Spacer between two halves of middle quad in medium beta triplet
 dmb45 drift 1mb46 - 1qmb4tot - 1qmb5tot - 1qmb5tot
 - 1dm56
 Drift between 4th and 5th quads in medium beta optics
 dmb56 drift ldm56
 Drift between 5th and 6th quads in medium beta optics
 dmbend drift ldmend
 Drift at ends of medium beta step

dmbmid drift lmbmid
 Drift at middle of medium beta step
 dmbstar drift lmbstar - lend
 Drift from medium beta IP to inner edge of triplet
 dsend drift lend + 0.5*lgds
 Drift replacing half a quad at the end of a dispersion suppressor
 dstep drift ldstep
 Drift separating up and down bends in the vertical steps
 dut12 drift ldut12
 Drift between 1st and 2nd quads in utility optics
 dut23 drift ldut23
 Drift between 2nd and 3rd quads in utility optics
 dut34 drift ldut34
 Drift between 3rd and 4th quads in utility optics
 dutstar drift loutstar - lend
 Drift from utility IP to inner edge of first quadrupole
 empty_dipole drift 2*lend + lbfield
 Drift to replace a dipole
 empty_slot drift lspoolel
 A vacant slot in a spool piece
 empty_spool drift lspoool
 An empty spool piece
 hgd90 quad -kquad90
 Half of the magnetic region in a D main arc quadrupole
 hqdsd quad -kquad90
 Half of the D dispersion suppressor quadrupole
 hqdsf quad kquad90
 Half of the F dispersion suppressor quadrupole
 hqf90 quad kquad90
 Half of the magnetic region in an F main arc quadrupole
 hqlbd1 quad -kqlb1
 Half of the 1st quad field (D) in a low beta triplet
 hqlbd2 quad -kqlb2
 Half of the 2nd quad field (D) in a low beta triplet
 hqlbd3 quad -kqlb3
 Half of the 3rd quad field (D) in a low beta triplet
 hqlbd4 quad -kqlb4

Half of the 4th quad field (D) in low beta optics
 hqlbd5 quad -kqlb5
 Half of the 5th quad field (D) in low beta optics
 hqlbd6 quad -kqlb6
 Half of the 6th quad field (D) in low beta optics
 hqlbf1 quad kqlb1
 Half of the 1st quad field (F) in a low beta triplet
 hqlbf2 quad kqlb2
 Half of the 2nd quad field (F) in a low beta triplet
 hqlbf3 quad kqlb3
 Half of the 3rd quad field (F) in a low beta triplet
 hqlbf4 quad kqlb4
 Half of the 4th quad field (F) in low beta optics
 hqlbf5 quad kqlb5
 Half of the 5th quad field (F) in low beta optics
 hqlbf6 quad kqlb6
 Half of the 6th quad field (F) in low beta optics
 hqmdl quad -kqmdl
 Half of the D quad field in "M = -1" sections
 hqmlf quad kqmdl
 Half of the F quad field in "M = -1" sections
 hqmbd1 quad -kqmb1
 Half of the 1st quad field (D) in a medium beta triplet
 hqmbd2 quad -kqmb2
 Half of the 2nd quad field (D) in a medium beta triplet
 hqmbd3 quad -kqmb3
 Half of the 3rd quad field (D) in a medium beta triplet
 hqmbd4 quad -kqmb4
 Half of the 4th quad field (D) in medium beta optics
 qmbd5 quad -kqmb5
 Half of the 5th quad field (D) in medium beta optics
 hqmbd6 quad -kqmb6
 Half of the 6th quad field (D) in medium beta optics
 hqmbf1 quad kqmb1
 Half of the 1st quad field (F) in a medium beta triplet
 hqmbf2 quad kqmb2
 Half of the 2nd quad field (F) in a medium beta triplet

hqmbf3 quad 0.5*lgmb3 kqmb3
 Half of the 3rd quad field (F) in a medium beta triplet
 hqmbf4 quad 0.5*lgmb4 kqmb4
 Half of the 4th quad field (F) in medium beta optics
 hqmbf5 quad 0.5*lgmb5 kqmb5
 Half of the 5th quad field (F) in medium beta optics
 hqmbf6 quad 0.5*lgmb6 kqmb6
 Half of the 6th quad field (F) in medium beta optics
 hqutd1 quad 0.5*lqut1 -kqut1
 Half of the 1st quad field (D) in utility optics
 hqutd2 quad 0.5*lqut2 -kqut2
 Half of the 2nd quad field (D) in utility optics
 hqutd3 quad 0.5*lqut3 -kqut3
 Half of the 3rd quad field (D) in utility optics
 hqutd4 quad 0.5*lqut4 -kqut4
 Half of the 4th quad field (D) in utility optics
 hqutf1 quad 0.5*lqut1 kqut1
 Half of the 1st quad field (F) in utility optics
 hqutf2 quad 0.5*lqut2 kqut2
 Half of the 2nd quad field (F) in utility optics
 hqutf3 quad 0.5*lqut3 kqut3
 Half of the 3rd quad field (F) in utility optics
 hqutf4 quad 0.5*lqut4 kqut4
 Half of the 4th quad field (F) in utility optics
 hspool drift 0.5*(lspool - 4*lspool) hspool
 Field free drifts at both ends of (idealised) spool pieces
 mds marker
 Marker at the ends of the dispersion suppressors
 miplbs marker
 Marker at the intersection point of the S low beta straight
 mipbt marker
 Marker at the intersection point of the T low beta straight
 mipby marker
 Marker at the intersection point of the Y medium beta straight
 mipbz marker
 Marker at the intersection point of the Z medium beta straight
 miputq marker
 Marker at the intersection point of the Q utility straight

miputr marker
 Marker at the intersection point of the R utility straight
 miputw marker
 Marker at the intersection point of the W utility straight
 miputx marker
 Marker at the intersection point of the X utility straight
 mlbstep marker
 Marker at ends of the low beta steps
 mmstep marker
 Marker at ends of the medium beta steps
 mq90 marker
 Marker at the center of every main arc quadrupole
 mqds marker
 Marker at center of dispersion suppressor quadrupoles
 mqjb marker
 Marker at the center of low beta quadrupoles
 mqml marker
 Marker at center of "M - 1" quadrupoles
 mqmb marker
 Marker at the center of medium beta quadrupoles
 mqut marker
 Marker at center of utility quadrupoles
 mtpoon marker
 Marker at the ends of CONVERGENT Transition Pieces
 mtdiv marker
 Marker at the ends of DIVERGENT Transition Pieces
 qtrimd quad lspool
 Defocussing trim quadrupole in spool pieces kqtrimd / lspool
 qtrimf quad lspool
 Focussing trim quadrupole in spool pieces kqtrimf / lspool
 sext_d sextupole lspool
 Sextupole in spool pieces at Defocussing locations ksd / lspool
 sext_f sextupole lspool
 Sextupole in spool pieces at Focussing locations ksf / lspool
 steer_d vkick lspool 0.0
 Vertical steering dipole, in spool pieces at D locations
 steer_f hkick lspool 0.0

Horizontal steering dipole, in spool pieces at F locations

- vsma marker
Virtual Survey Marker near the center of sector A
- vsmb marker
Virtual Survey Marker near the center of sector B
- vsmc marker
Virtual Survey Marker near the center of sector C
- vsmd marker
Virtual Survey Marker near the center of sector D
- vsme marker
Virtual Survey Marker near the center of sector E
- vsmf marker
Virtual Survey Marker near the center of sector F
- vsmg marker
Virtual Survey Marker near the center of sector G
- vsmh marker
Virtual Survey Marker near the center of sector H

***** STRENGTH *****

Section 4

Format:

| Strength parameter name | Definition |
|--|--------------|
| qqlb1 | kqlb1 * brho |
| Gradient of 1st low beta quad (collision optics) [T/m] | |
| qqlb2 | kqlb2 * brho |
| Gradient of 2nd low beta quad (collision optics) [T/m] | |
| qqlb3 | kqlb3 * brho |
| Gradient of 3rd low beta quad (collision optics) [T/m] | |
| qqlb4 | kqlb4 * brho |
| Gradient of 4th low beta quad (collision optics) [T/m] | |
| qqlb5 | kqlb5 * brho |
| Gradient of 5th low beta quad (collision optics) [T/m] | |
| qqlb6 | kqlb6 * brho |
| Gradient of 6th low beta quad (collision optics) [T/m] | |
| qqlm1 | kqml * brho |

Gradient of the "M = -1" section quadrupole [T/m]

- qgmb1 kqmb1 * brho
Gradient of 1st medium beta quad (collision optics) [T/m]
- qgmb2 kqmb2 * brho
Gradient of 2nd medium beta quad (collision optics) [T/m]
- qgmb3 kqmb3 * brho
Gradient of 3rd medium beta quad (collision optics) [T/m]
- qgmb4 kqmb4 * brho
Gradient of 4th medium beta quad (collision optics) [T/m]
- qgmb5 kqmb5 * brho
Gradient of 5th medium beta quad (collision optics) [T/m]
- qgmb6 kqmb6 * brho
Gradient of 6th medium beta quad (collision optics) [T/m]
- qgtrimd kqtrimd * brho
Integrated strength of trim D quads in spool pieces [T]
- qgtrimf kqtrimf * brho
Integrated strength of trim F quads in spool pieces [T]
- qquad90 kquad90 * brho
Gradient of main arc quadrupoles [T/m]
- qgut1 kgut1 * brho
Gradient of 1st utility quad [T/m]
- qgut2 kgut2 * brho
Gradient of 2nd utility quad [T/m]
- qgut3 kgut3 * brho
Gradient of 3rd utility quad [T/m]
- qgut4 kgut4 * brho
Gradient of 4th utility quad [T/m]
- gsd ksd * brho
Integrated strength of D sextupoles in spool pieces [T/m]
- gsf ksf * brho
Integrated strength of F sextupoles in spool pieces [T/m]
- kqlb1 .002842520
Normalised strength of 1st low beta quad (collision optics) [m**-2]
- kqlb2 .003386201
Normalised strength of 2nd low beta quad (collision optics) [m**-2]
- kqlb3 .003420626
Normalised strength of 3rd low beta quad (collision optics) [m**-2]

kqlb4 .002614959
 Normalised strength of 4th low beta quad (collision optics) [m**2]
 kqlb5 .00002969583
 Normalised strength of 5th low beta quad (collision optics) [m**2]
 kqlb6 .00194640
 Normalised strength of 6th low beta quad (collision optics) [m**2]
 kgml .0031772752
 Normalised strength of the "M - 1" section quadrupoles [m**2]
 kgmb1 .002622310
 Normalised strength of 1st medium beta quad (collision optics) [m**2]
 kgmb2 .002688887
 Normalised strength of 2nd medium beta quad (collision optics) [m**2]
 kgmb3 .002631694
 Normalised strength of 3rd medium beta quad (collision optics) [m**2]
 kgmb4 .001997400
 Normalised strength of 4th medium beta quad (collision optics) [m**2]
 kgmb5 .0005467249
 Normalised strength of 5th medium beta quad (collision optics) [m**2]
 kgmb6 .002766228
 Normalised strength of 6th medium beta quad (collision optics) [m**2]
 kqtrim 0.0
 Integrated normalised strength of trim D quads in spool pieces [m**1]
 kqtrimf 0.0
 Integrated normalised strength of trim F quads in spool pieces [m**1]
 kquad90 0.00315353
 Normalised strength of main arc quadrupoles [m**2]
 kqut1 .00254224
 Normalised strength of 1st utility quad [m**2]
 kqut2 .00254224
 Normalised strength of 2nd utility quad [m**2]
 kqut3 .0031778
 Normalised strength of 3rd utility quad [m**2]
 kqut4 .0031778
 Normalised strength of 4th utility quad [m**2]
 ksd 0.0
 Integrated normalised strength of D sextupoles in spool pieces [m**2]
 ksf 0.0
 Integrated normalised strength of F sextupoles in spool pieces [m**2]

Section 5 GEOMETRY

Format:

Geometry parameter name Definition
 Comment

bangl 2.0 * pi / ndipoles
 Bend angle per dipole
 bbvlb1 5.08149728
 Vertical bending field in inner low beta step [Tesla]
 bbvlb2 6.5453343
 Vertical bending field in outer low beta step [Tesla]
 bbvmb 5.2119375
 Vertical bending field in medium beta step [Tesla]
 bfield brho / rho
 Magnetic field required in dipoles for closure [Tesla]
 brho energy / clight
 Magnetic rigidity, [Tesla metres]
 cells_per_endsec J1
 The number of cells in a beginning arc sector
 cells_per_sector 36
 The nominal number of cells per main arc sector
 clight 2.99792458e8
 The speed of light [metres/second]
 dipoles_per_hcell 6
 The number of dipoles per main arc half cell
 energy 2.0e13
 Energy of circulating beam [eV] (strictly speaking, momentum in [eV/c])
 lbfield 16.54
 Magnetic length of main arc dipole field [metres]
 lbpm 0.2
 Length of a Beam Position Monitor [metres]
 lbvlb1 5.0
 Length of vertical bend fields in inner low beta step [metres]
 lbvmb 8.0
 Length of vertical bend fields in medium beta steps [metres]

ldipole lbfield + 2*lend
Physical length of a standard dipole [metres]

ldlblend 7.0875
Length of drift at ends of inner low beta step [m]

ldlblmid 217.95
Length of drift at middle of inner low beta step [m]

ldlb2 0.05
Length of drift between two halves of 2nd quad in low beta triplet [m]

ldlb2end $0.5 * (ldml - 4.0) - 0.6$
Length of drift at ends of outer low beta step [m]

ldlb2amid 19.04
Length of drift in middle of outer low beta step

ldlb56 8.2
Length of drift between 5th and 6th low beta quadrupoles [m]

ldml $0.5 * lhmlcell - (lqml + 2*lend)$
Length of drift on either side of "M = -1" quads [m]

ldmb2 8.85
Drift between halves of middle quadrupole in medium beta triplet [m]

ldmb56 8.2
Length of drift between 5th and 6th medium beta quadrupoles [m]

ldmbend 24.9625
Length of drift at ends of medium beta step [m]

ldmbmid 34.2
Length of drift at middle of medium beta step [m]

lds1a 4.92149
Length of drift before dipoles in 1st half cell in DS (m)

lds2a 5.40643
Length of drift before dipoles in 2nd half cell in DS (m)

lds3a 5.02576
Length of drift before dipoles in 3rd half cell in DS (m)

lds4a 5.52739
Length of drift before dipoles in 4th half cell in DS (m)

ldsfree lhdsceil - (lqds+2*lend) - 4*(lbfieid+2*lend)
Total free space at either end of dipoles in a dispersion suppressor half cell

ldstep 0.2
Length of silly drift between dipoles in vertical bends [m]

ldut12 .1994

Length of drift between 1st and 2nd utility quadrupoles [m]

ldut23 199.1848
Length of drift between 2nd and 3rd utility quadrupoles [m]

ldut34 4.7204
Length of drift between 3rd and 4th utility quadrupoles [m]

lend 0.4
Length of the field free region at both ends of all(?) magnets [metres]

lhceil dipoles_per_hceil*ldipole + lquad + lspool
Length of a main arc half cell [metres]

lhdsceil $0.75 * lhceil$
Length of a dispersion suppressor half cell [metres]

lhmlceil 37.5
Length of half an "M = -1" cell [m]

lhqds0 1.81971
Magnetic length of the standard dispersion suppressor quads [m]

llb46 71.0
Length from inner face of 4th low beta quad to outside of 6th [m]

llbstar 21.76
Length from low beta IP to 1st quadrupole FIELD [m]

lmb46 67.0
Length from inner face of 4th medium beta quad to outside of 6th [m]

lmbstar 121.76
Length from medium beta IP to 1st quadrupole FIELD [m]

lqds 5.33048
Magnetic length of dispersion suppressor quads [m]

lqfield 3.96
Magnetic length of the standard main arc quadrupoles [metres]

lqlb1 16.4
Magnetic length of 1st low beta quad [m]

lqlb2 11.0
Magnetic length of 2nd low beta quad [m]

lqlb3 12.4
Magnetic length of 3rd low beta quad [m]

lqlb4 10.0
Magnetic length of 4th low beta quad [m]

lqlb4tot lqlb4 + 2*lend
Total length of 4th low beta quadrupole

lqlb5 12.0
 Magnetic length of 5th low beta quad [m]
 lqlb5tot lqlb5 + 2*lend
 Total length of 5th low beta quadrupole
 lqlb6 6.0
 Magnetic length of 6th low beta quad [m]
 lqlb6tot lqlb6 + 2*lend
 Total length of 6th low beta quadrupole
 lqml 12.32
 Magnetic length of "M - 1" quad [m]
 lqmb1 10.0
 Magnetic length of 1st medium beta quad [m]
 lqmb2 10.0
 Magnetic length of 2nd medium beta quad [m]
 lqmb3 12.0
 Magnetic length of 3rd medium beta quad [m]
 lqmb4 12.0
 Magnetic length of 4th medium beta quad [m]
 lqmb4tot lqmb4 + 2*lend
 Total length of 4th medium beta quadrupole
 lqmb5 6.0
 Magnetic length of 5th medium beta quad [m]
 lqmb5tot lqmb5 + 2*lend
 Total length of 5th medium beta quadrupole
 lqmb6 4.0
 Magnetic length of 6th medium beta quad [m]
 lqmb6tot lqmb6 + 2*lend
 Total length of 6th medium beta quadrupole
 lquad lqfield + 2*lend + lbpm
 Physical length of a main arc quadrupole (metres)
 lqut1 10.646
 Magnetic length of 1st utility quad [m]
 lqut2 11.7204
 Magnetic length of 2nd utility quad [m]
 lqut3 7.2978
 Magnetic length of 3rd utility quad [m]
 lqut4 8.3996
 Magnetic length of 4th utility quad [m]

lspool 5.57
 Physical length of the main arc "spool piece" correction packages [metres]
 lspole1 0.001
 Magnetic length of (idealised) spool piece correction elements [metres]
 lutstar 384.7667
 Length from utility IP to 1st utility quadrupole [m]
 ndipoles 3848
 Total number of dipoles in the SSC main ring
 pi 3.14159265359
 The well known geometric constant
 rho (ndipoles*lbfield) / (2.0*pi)
 Radius of curvature in the dipoles [metres]

Section 6 NAME_LOCATION

Format:

| Object name | Table location |
|------------------|----------------|
| bangl | geometry |
| bbv1b1 | geometry |
| bbv1b2 | geometry |
| bbvmb | geometry |
| bdowmb1 | magnet_piece |
| bdowmb2 | magnet_piece |
| bdowmb | magnet_piece |
| bds1 | beam_line |
| bds2 | beam_line |
| bds3 | beam_line |
| bds4 | beam_line |
| bend | magnet_piece |
| bfield | geometry |
| bpm | magnet_piece |
| brho | geometry |
| bup1b1 | magnet_piece |
| bup1b2 | magnet_piece |
| bupmb | magnet_piece |
| celldd | beam_line |
| celiff | beam_line |
| cells_per_endsec | geometry |
| cells_per_sector | geometry |
| clight | geometry |
| converge | beam_line |
| d_w | beam_line |
| ddsla | magnet_piece |
| ddslb | magnet_piece |

miplbt magnet_piece
 mlpmbz magnet_piece
 mipmbz magnet_piece
 miputq magnet_piece
 miputr magnet_piece
 miputw magnet_piece
 miputx magnet_piece
 mlbstep magnet_piece
 mlbstep magnet_piece
 mq90 magnet_piece
 mqds magnet_piece
 mqdb magnet_piece
 mqml magnet_piece
 mqnb magnet_piece
 mqut beam_line
 mftod magnet_piece
 mtpoon magnet_piece
 mtpdiv magnet_piece
 ndipoles geometry
 near beam_line
 pi geometry
 q_r beam_line
 qdsd ideal_magnet
 qdsf ideal_magnet
 qhybd ideal_magnet
 qhybf ideal_magnet
 qlbd1 ideal_magnet
 qlbd2 ideal_magnet
 qlbd3 ideal_magnet
 qlbd4 ideal_magnet
 qlbd5 ideal_magnet
 qlbd6 ideal_magnet
 qlbf1 ideal_magnet
 qlbf2 ideal_magnet
 qlbf3 ideal_magnet
 qlbf4 ideal_magnet
 qlbf5 ideal_magnet
 qlbf6 ideal_magnet
 qml d
 qmlf ideal_magnet
 qmbd1 ideal_magnet
 qmbd2 ideal_magnet
 qmbd3 ideal_magnet
 qmbd4 ideal_magnet
 qmbd5 ideal_magnet
 qmbd6 ideal_magnet
 qmbf1 ideal_magnet
 qmbf2 ideal_magnet
 qmbf3 ideal_magnet
 qmbf4 ideal_magnet
 qmbf5 ideal_magnet
 qmbf6 ideal_magnet
 qtrimd magnet_piece
 qtrimf ideal_magnet
 quad90d ideal_magnet
 quad90f ideal_magnet

qutd1 ideal_magnet
 qutd2 ideal_magnet
 qutd3 ideal_magnet
 qutd4 ideal_magnet
 qutf1 ideal_magnet
 qutf2 ideal_magnet
 qutf3 ideal_magnet
 qutf4 ideal_magnet
 r_s beam_line
 rho geometry
 right beam_line
 s_t beam_line
 sector_a beam_line
 sector_b beam_line
 sector_c beam_line
 sector_d beam_line
 sector_e beam_line
 sector_f beam_line
 sector_g beam_line
 sector_h beam_line
 sext_d magnet_piece
 sext_f magnet_piece
 spoold ideal_magnet
 spoolf ideal_magnet
 ssc_red beam_line
 steer_d magnet_piece
 steer_f magnet_piece
 step_d_lbl beam_line
 step_d_lbl2 beam_line
 step_d_mb beam_line
 step_u_lbl beam_line
 step_u_lbl2 beam_line
 step_u_mb beam_line
 strait_q beam_line
 strait_r beam_line
 strait_s beam_line
 strait_t beam_line
 strait_w beam_line
 strait_x beam_line
 strait_y beam_line
 strait_z beam_line
 t_a beam_line
 up_lbl beam_line
 up_lbl2 beam_line
 up_mb beam_line
 utility_d beam_line
 utility_f beam_line
 vsmua magnet_piece
 vsmvb magnet_piece
 vsmc magnet_piece
 vsmd magnet_piece
 vsme magnet_piece
 vsmf magnet_piece
 vsmg magnet_piece
 vsmh magnet_piece
 w_x beam_line

x_y
y_z
z_e

beam_line
beam_line
beam_line